22. Cannon, R. Q. *Highlights of Astronomy* Vol. 6 (ed. West, R. M.) 109–117 (Reidel, Dordrecht, 1983).
23. Rowan-Robinson, M. *The Cosmological Distance Ladder* (Freeman, New York, 1985).
24. Fukugita, M., Hogan, C. J. & Peebles, P. J. E. *Nature* **366,** 309–312 (1993).
25. Walker, T. P. *et al. Astrophys. J.* **376,** 51–69 (1991).
26. Gott, J. R., Gunn, J. E., Schramm, D. N. & Tinsley, B. M. *Astrophys. J.* **194,** 543–553 (1974).
27. White, S. D. M., Navarro, J. F., Evrard, A. E. & Frenk, C. S. *Nature* **366,** 429–433 (1933).
28. Hogan, C. J. *Ann. N. Y. Acad. Sci.* **647,** 76–85 (1991).
29. Sandage, A. R. *Phys. Today* **23,** 34–43 (1967).
30. Kellerman, K. I. *Nature* **361,** 134–136 (1993).
31. Fahlman, G., Kaiser, N., Squires, G. & Woods, D. *Astrophys. J.* (in the press).
32. Tyson, J. A., Valdes, F. & Wenk, R. A. *Astrophys. J.* **349,** L1–L4 (1990).
33. Gardner, J. P., Cowie, L. L. & Wainscoat, R. J. *Astrophys. J.* **415,** 9–12 (1993).
34. Kaiser, N. *Astrophys. J.* **284,** L9–L12 (1984).
35. Rees, M. J. *Mon. Not. R. astr. Soc.* **213,** 75P–81P (1985).
36. Dekel, A. *Comments Astrophys.* **11,** 235–256 (1986).
37. Bardeen, J. M., Bond, J. R., Kaiser, N. & Szalay, A. S. *Astrophys. J.* **304,** 15–61 (1986).
38. Dekel, A. & Rees, M. J. *Nature* **326,** 455–462 (1987).
39. Coles, P. *Mon. Not. R. astr. Soc.* **262,** 1065–1075 (1993).
40. Babul, A. & White, S. D. M. *Mon. Not. R. astr. Soc.* **253,** 31P–34P (1991).
41. Bower, R. G., Coles, P., Frenk, C. S. & White, S. D. M. *Astrophys. J.* **405,** 403–412 (1993).
42. Maddox, S. J., Efstathiou, G., Sutherland, W. J. & Loveday, J. A. *Mon. Not. R. astr. Soc.* **242,** 43P–47P (1990).
43. Collins, C. A., Nichol, R. C. & Lumsden, S. L. *Mon. Not. R. astr. Soc.* **254,** 295–300 (1992).
44. Efstathiou, G., Sutherland, W. J. & Maddox, S. J. *Nature* **348,** 705–707 (1990).
45. Efstathiou, G. *et al. Mon. Not. R. astr. Soc.* **247,** 10P–14P (1990).
46. Saunders, W. *et al. Nature* **349,** 32–38 (1991).
47. Peacock, J. A. *Mon. Not. R. astr. Soc.* **253,** 1P–4P (1991).
48. Peacock, J. A. & Dodds, S. J. *Mon. Not. R. astr. Soc.* **267,** 1020–1034 (1994).
49. Davis, M. & Peebles, P. J. E. *Astrophys. J.* **267,** 465–482 (1983).
50. Bean, A. J., Efstathiou, G., Ellis, R. S., Peterson, B. A. & Shanks, T. *Mon. Not. R. astr. Soc.* **205,** 605–624 (1983).
51. Peebles, P. J. E. *Science* **224,** 1385–1391 (1984).
52. Hale-Sutton, D., Fong, R., Metcalfe, N. & Shanks, T. *Mon. Not. R. astr. Soc.* **237,** 569–587 (1989).
53. Tully, R. B. *Astrophys. J.* **321,** 280–304 (1987).
54. Fisher, K. B., Davis, M., Strauss, M. A., Yahil, A. & Huchra, J. P. *Mon. Not. R. astr. Soc.* **267,** 927–948 (1994).
55. Jones, C. & Forman, W. *Astrophys. J.* **276,** 38–55 (1984).
56. Richstone, D. O. & Tremaine, S. *Astr. J.* **92,** 72–74 (1986).
57. Persic, M. & Salucci, P. *Mon. Not. R. astr. Soc.* **234,** 131–154 (1988).
58. Persic, M. & Salucci, P. *Mon. Not. R. astr. Soc.* **245,** 577–581 (1990).
59. Burstein, D. *Rep. Prog. Phys.* **53,** 421–481 (1990).
60. Bertschinger, E. & Dekel, A. *Astrophys. J.* **336,** L5–L8 (1989).
61. Dekel, A., Bertschinger, E. & Faber, S. M. *Astrophys. J.* **364,** 349–369 (1990).
62. Dekel, A. *et al. Astrophys. J.* **412,** 1–21 (1993).
63. Bertschinger, D., Dekel, A., Faber, S. M. & Burstein, D. *Astrophys. J.* **364,** 370–395 (1990).
64. Silk, J. *Astrophys. J.* **345,** L1–L4 (1989).
65. Guzman, R. & Lucey, J. R. *Mon. Not. R. astr. Soc.* **263,** L47–L50 (1993).
66. Lubin, P. M., Epstein, G. L. & Smoot, G. F. *Phys. Rev. Lett.* **50,** 616–619 (1983).
67. Strauss, M. & Davis, M. in *Proceedings of Vatican Study Week on Large-scale Motions in the Universe* (eds Rubin, V. C. & Coyne, G.) 256–277 (Princeton Univ. Press, USA, 1988).
68. Rowan-Robinson, M. *et al. Mon. Not. R. astr. Soc.* **247,** 1–18 (1990).
69. Scaramella, R., Vettolani, G. & Zamorani, G. *Astrophys. J.* **376,** L1–L4 (1991).
70. Plionis, M. & Valdarnini, R. *Mon. Not. R. astr. Soc.* **249,** 46–61 (1991).
71. Plionis, M., Coles, P. & Catelan, P. *Mon. Not. R. astr. Soc.* **262,** 465–474 (1993).
72. Hudson, M. J. *Mon. Not. R. astr. Soc.* **265,** 72–80 (1993).
73. Lauer, T. R. & Postman, M. *Astrophys. J.* **425,** 418–438 (1994).
74. Kaiser, N. *Mon. Not. R. astr. Soc.* **227,** 1–21 (1987).
75. Hogan, C. J., Kaiser, N. & Rees, M. J. *Phil. Trans. R. Soc.* A**307,** 97–109 (1982).
76. Kaiser, N. & Silk, J. *Nature* **324,** 529–537 (1987).
77. Smoot, G. F. *et al. Astrophys. J.* **396,** L1–L5 (1992).
78. Hancock, S. *et al. Nature* **367,** 333–338 (1994).
79. Wright, E. L. *et al. Astrophys. J.* **396,** L13–L18 (1992).
80. Stoeger, W. R., Ellis, G. F. R. & Xu, C. *Phys. Rev.* D**49,** 1845–1853 (1994).
81. Ellis, G. F. R. & Tavakol, R. *Class. Qu. Grav.* **11,** 675–688 (1994).
82. Traschen, J. E. & Eardley, D. M. *Phys. Rev.* D**34,** 1665–1679 (1986).
83. Holtzman, J. *Astrophys. J. Suppl. Ser.* **71,** 1–24 (1989).
84. Gouda, N., Sugiyama, N. & Sasaki, M. *Astrophys. J.* **372,** L49–L52 (1991).
85. Wilson, M. L. *Astrophys. J.* **273,** 2–15 (1983).
86. Kamionski, M. & Spergel, D. N. *Astrophys. J.* (in the press).
87. Peebles, P. J. E., Schramm, D. N., Turner, E. L. & Kron, R. G. *Nature* **352,** 769–776 (1991).

ACKNOWLEDGEMENTS. We thank D. W. Sciama, P. Salucci, C. J. Hogan, C. J. Isham and, particularly, P. J. E. Peebles for comments; and M. Plionis for preparing Fig. 2 and for comments. P.C. received a SERC Advanced Research fellowship. We both thank the SERC for support under the QMW Visitor's Programme, and G.F.R.E. thanks the FRD (South Africa) for financial support.

ARTICLES

Controlling chaos in the brain

Steven J. Schiff*, Kristin Jerger*, Duc H. Duong*, Taeun Chang*, Mark L. Spano† & William L. Ditto‡

* Department of Neurosurgery, Children's National Medical Center
and The George Washington University School of Medicine, Washington DC 20010, USA
† Naval Surface Warfare Center, White Oak Laboratory, Silver Spring, Maryland 20903, USA
‡ School of Physics, Georgia Institute of Technology, Atlanta, Georgia 30332, USA

In a spontaneously bursting neuronal network *in vitro*, chaos can be demonstrated by the presence of unstable fixed-point behaviour. Chaos control techniques can increase the periodicity of such neuronal population bursting behaviour. Periodic pacing is also effective in entraining such systems, although in a qualitativeiy different fashion. Using a strategy of anticontrol such systems can be made less periodic. These techniques may be applicable to *in vivo* epileptic foci.

FOLLOWING the recent theoretical prediction that chaotic physical systems might be controllable with small perturbations[1,2], there has been rapid and successful application of this technique to mechanical systems[3], electrical circuits[4], lasers[5] and chemical reactions[6,7]. Following the demonstration of the control of chaos in arrhythmic cardiac tissue[8], there are no longer any technical barriers to applying these techniques to neural tissue.

One of the hallmarks of the human epileptic brain during periods of time in between seizures is the presence of brief bursts of focal neuronal activity known as interictal spikes. Often such spikes emanate from the same region of brain from which the seizures are generated but the relationship between the spike patterns and seizure onsets remains unclear[9,10]. Several types of *in vitro* brain slice preparations, usually after exposure to convulsant drugs that reduce neuronal inhibition, exhibit population burst-firing activity that in many ways seems analogous to the interictal spike[11]. One of these preparations is the high potassium concentration ($[K^+]$) model, where slices from the hippocampus of the temporal lobe of the rat brain (a frequent site of epileptogenesis in the human) are exposed to artificial cerebrospinal fluid containing 6.5–10 mM $[K^+]$[12]. After exposure to high $[K^+]$, spontaneous bursts of synchronized neuronal activity originate in a region known as the third part of the cornu ammonis or CA3 (ref. 13). Impulses from the CA3 bursts are propagated through a recurrent collateral fibre tract (the Schaffer collateral fibres) from CA3 to CA1, where electrographic seizure-like discharges can frequently be

observed[14]. A detailed computer model of the high [K^+] burst discharges in CA3 successfully replicates many of the experimental findings[15] (reviewed in ref. 16). Although it is difficult to identify determinism in long time series of such bursting activity using nonlinear prediction techniques, some evidence of determinism was recently identified[17,18]. We sought to determine whether such neuronal bursting activity was amenable to control.

There have been substantial efforts to influence neuronal activity with electric fields and currents. Regarding the *in vitro* hippocampal slice, brief direct current (d.c.) currents from nonpolarizable electrodes in the perfusion bath can influence the evoked excitability of pyramidal cells in normal [K^+] when the electric fields are suitably oriented[19]. Apparently similar effects can be achieved with brief currents from monopolar polarizable microelectrodes placed directly into the tissue[20,21]. To our knowledge the use of electrical stimulation to entrain spontaneous burst discharges from CA3 in high [K^+] has not been attempted, whether indirectly with electric fields or with direct stimulation of the nerve cells themselves. Direct stimulation can be accomplished for CA3 neurons by stimulating the Mossy fibre neurons that synapse on the CA3 pyramidal cells (orthodromic stimulation) or by stimulating branches of the CA3 pyramidal cell axons (Schaffer collateral fibres) and allowing the action potentials to propagate into the pyramidal cells in a retrograde fashion (antidromic stimulation).

With the observation that it was feasible to entrain burst discharges from CA3 with both orthodromic and antidromic stimulation (K.J. and S.J.S., manuscript in preparation), we were in a position to ask the following questions: (1) is there evidence for deterministic chaotic behaviour in this preparation; and (2) could such activity be controlled?

If one observes the timing of events from a chaotic physical system, those events are aperiodic. The timing of events evolves from one unstable periodicity to another. Furthermore the approach to these unstable periodicities shows recurring patterns

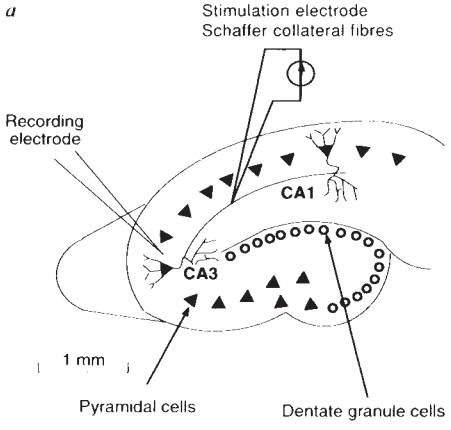

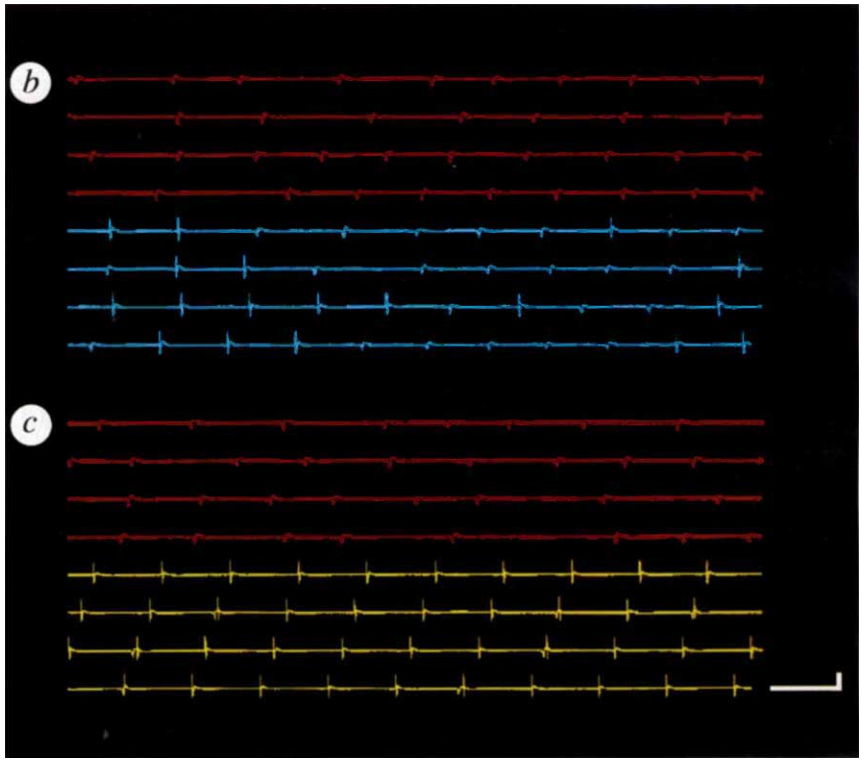

FIG. 1 *a*, Schematic diagram of the transverse hippocampal slice, and arrangement of recording electrodes. Female Sprague–Dawley rats weighing 125–150 g were anaesthetized with diethyl-ether and decapitated. Transverse slices 400 μm thick were prepared from the hippocampus with a tissue chopper and placed in an interface-type perfusion chamber at 32–35 C. Slices were perfused with artificial cerebrospinal fluid (ACSF) flowing at 2 ml min^{-1} and composed of 155 mM Na^+, 136 mM Cl^-, 3.5 mM K^+, 1.2 mM Ca^{2+}, 1.2 mM Mg^{2+}, 1.25 mM PO_4^{2-}, 24 mM HCO_3^-, 1.2 mM SO_4^{2-}, and 10 mM dextrose. After 90 min of incubation, slices were tested for viability by recording a greater than 2 mV unitary population spike in the stratum pyramidale of CA1, in response to stimulation of Schaffer collateral fibres in the stratum radiatum with 100 μs constant current 50–150 μA square-wave pulses delivered at 0.1 Hz through tungsten microelectrodes. Recordings were made with 2–4-MΩ glass needle electrodes filled with 150 mM NaCl. With confirmation of viability, the perfusate was switched to ACSF containing 8.5 mM [K^+] and 141 mM [Cl^-]. After 15–20 min of high [K^+] perfusion, spontaneous burst firing could be recorded from CA3a or CA3b. Recordings were digitized across 12 bits at 5 kHz with a Digidata 1200 analogue to digital converter (Axon Instruments), and stored on a personal computer using Axotape 2.0 (Axon Instruments). CA3 interburst intervals were measured with Datapac II (Run Technologies). For control purposes, a separate computer system, digitizing across 16 bits at 1 kHz, identified spontaneous bursts from CA3 using a threshold and peak amplitude detection strategy. This computer triggered a stimulator (Model S8800, Grass Corp.) linked to a photoelectric stimulus isolation unit (Model SIU7, Grass Corp.), to deliver 100-μs constant current square-wave pulses to the Schaffer collateral fibres through a tungsten microelectrode. At times, double pulses consisting of pairs of 100-μs pulses with 150-μs interpulse intervals were used. *b*, Shown are 100 s of recording from an extracellular electrode within CA3 following exposure to 8.5 mM [K^+]. The upper four traces in red show the burst discharges occurring at irregular intervals. The lower four traces in blue show the effect of turning on chaos control. When control of chaos pulses are delivered to the Schaffer collateral fibres, large stimulation artefacts are seen at the onset of a burst. Note that each control pulse evokes a synchronized discharge in CA3. As control becomes more stable, the bursts become increasingly periodic, as seen most clearly on the bottom trace. Note that the control pulses are delivered only intermittently. The plot of the full series of these intervals before and during control is seen in the first half of the plot in Fig. 3. *c*, Shown are 100 s of recording from the same experiment before (red) and after (yellow) the initiation of periodic pacing. Note that periodic pulses immediately entrain the population bursts in the fifth tracing (10/10 pulses), but by the sixth tracing, there is occasional escape behaviour evident when the population bursts just before the delivered pulse (seen in 3/10 bursts in tracing 6, 2/11 in tracing 7, and 2/10 in tracing 8). The plot of the full series of these intervals before and during periodic pacing is seen in the second half of the plot in Fig. 3. The calibration mark indicates 5 mV ordinate and 1 s abscissa.

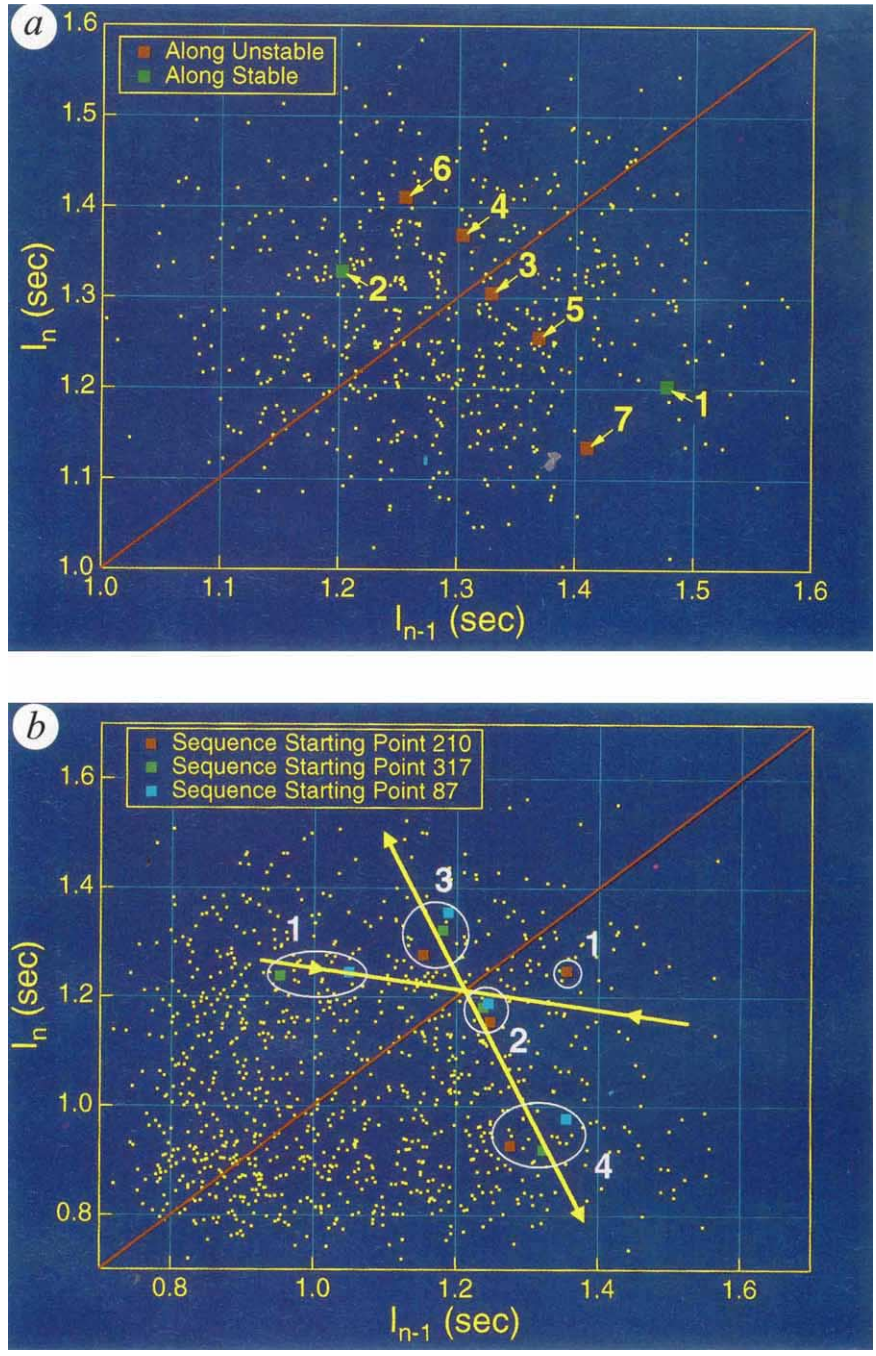

FIG. 2 *a*, Return plots of interburst intervals I_n versus the previous interval I_{n-1} without control. Seven sequential points are colour coded and numbered 1–7. Note that as the trajectory crosses the line of identity along a particular direction from 1 to 2, the next points take a peculiar sequence that starts close to the line of identity at point 3, and then alternates on either side of the line of identity and progressively diverges from it along a nearly straight line for points 3–7. The points coloured in green (1, 2), define a stable direction or manifold, whereas the points in red (3–7) define an unstable manifold. The intersection of these manifolds with the line of identity defines the unstable fixed point. Note that, as for other physical and biological systems[3,8], the saddle observed in these preparations is a flip saddle; that is, while the distances of successive state points from the fixed point increase in an exponential fashion along the unstable manifold, the state points alternate on opposite sides of the line of identity. *b*, Return plot showing multiple colour-coded trajectories that did not follow each other in time. The starting point for each sequence, numbered 1 in each, began at burst numbers 87 (blue), 210 (red) and 317 (green), out of a total series of 320 bursts. The stable manifold is shown with arrows pointing towards the unstable fixed point, and the unstable manifold has arrows drawn in the direction away from the unstable fixed point. Note that each sequence starts at a point roughly the same distance from the unstable fixed point in a region close to the stable manifold. Each trajectory follows roughly the same path, and after closely approaching the unstable fixed point for the points labelled 2 (red, green and blue), there evolves for each trajectory a sequence of exponentially diverging jumps (on alternating sides of the line of identity along the unstable manifold). Although the trajectories are clustered along the unstable manifold for four bursts, the fifth bursts are widely scattered (not shown). This is the manifestation of the sensitivity to initial conditions typical of chaotic systems. These plots show clear evidence for non-random structure in these trajectories, and their patterns bear the hallmarks of deterministic chaos.

which can be quantitatively understood by examining the relationship between the timing of sequential events. This can be visualized using a plot which is a type of a return map. Such a map plots the present interval between events, I_n, versus the jth previous interval, I_{n-j}. Periodicities (of period j) are revealed on such a plot as intersections with the line of identity, $I_n = I_{n-j}$. In a chaotic system these intersections are known as unstable fixed points. These unstable fixed points are deterministically approached from a direction called the stable direction or manifold and exponentially diverge from these points along the unstable direction or manifold. This type of local geometry has the shape of a saddle. Chaos control[1,3,8] consists of the identification and characterization of these saddles, followed by a control intervention which exploits the local geometry of the saddle to increase the periodic behaviour of the system.

We demonstrate here three separate approaches to control: periodic pacing, an implementation of chaos control theory, and the inverse of chaos control which we term anticontrol.

Brain slice preparation

Hippocampal slices were prepared using standard techniques[18]. Glass micropipette electrodes in CA1 and CA3 were used to record neuronal activity, and a computer calculated and delivered appropriately timed control pulses. The anatomy of the transverse hippocampal slice and arrangement of electrodes are illustrated in Fig. 1*a*, and details of the experimental preparation are summarized in the figure legend.

Chaos identification and control

A key feature of chaotic systems is that they contain an infinite number of unstable periodic fixed points[22]. That these spontaneously active neuronal networks are chaotic was supported by evidence of unstable fixed points in the return maps with the characteristics shown in Fig. 2*a*, *b*. These candidate unstable fixed points met four criteria. First, the sequence of points approaches the unstable fixed-point candidate along a stable direction and diverges from it along an unstable direction.

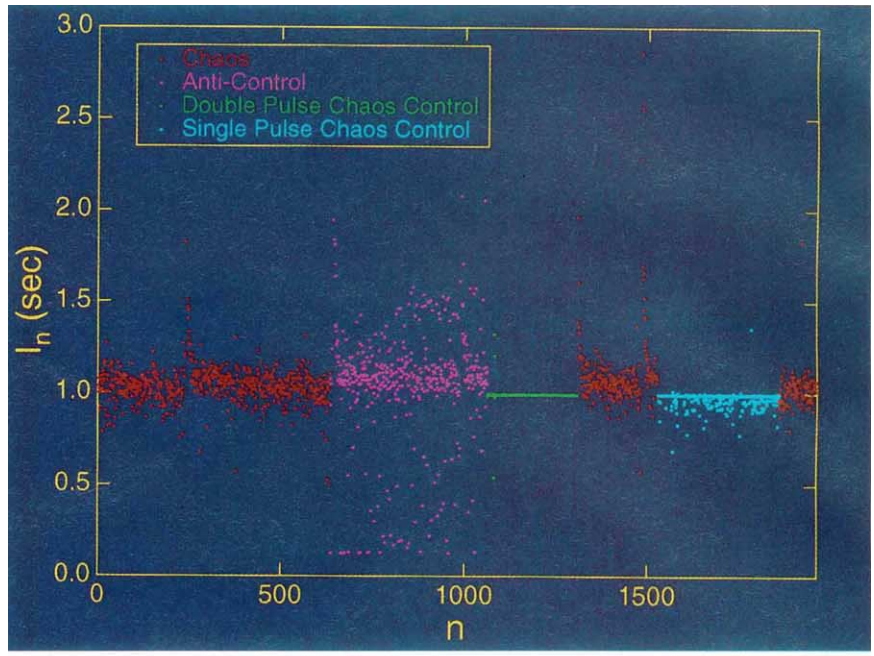

FIG. 3 Plot showing chaotic (red) interburst intervals I_n before and after single-pulse chaos control (blue) and single-pulse periodic pacing (yellow). Burst number is indicated by n. Note the qualitative differences in the control achieved with each method. Raw data from the onsets of chaos control and periodic pacing are shown in Fig. 1*b*, *c*.

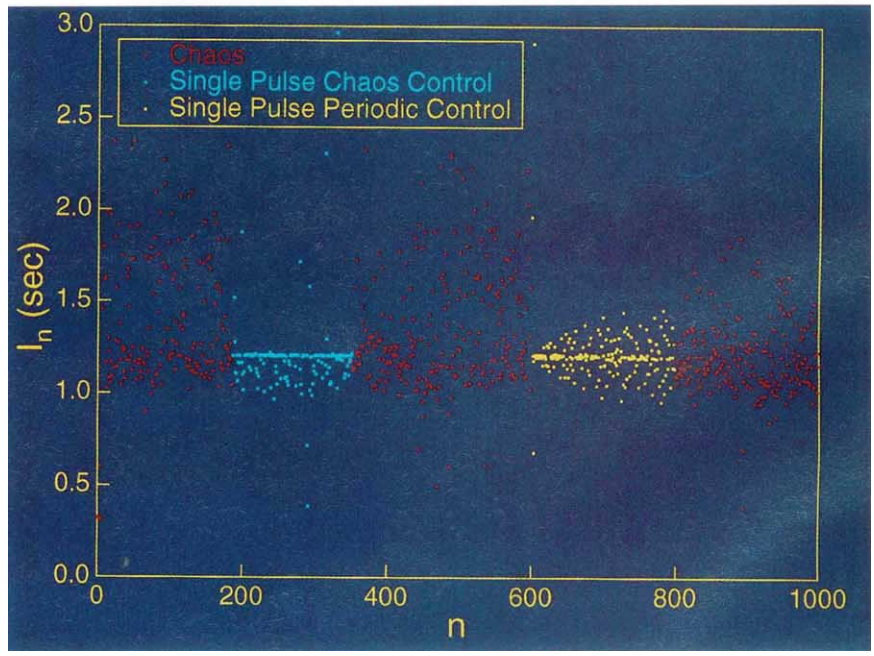

FIG. 4 Comparison of anticontrol (pink), double-pulse chaos control (green) and single-pulse control (blue). Note how anticontrol reduces the periodicity of the preparation. Also note that double-pulse control is more effective than single-pulse control, as was generally the case (see Table 1).

Second, the departing trajectory must be locally linear. Third, multiple approaches to the same candidate along the same stable direction with the corresponding departures along the same unstable direction must be detected. Last, the distances of the departing points from the candidate fixed point must increase exponentially, thereby demonstrating the sensitivity to initial conditions that is the defining feature of chaos. Although short single approaches to candidate unstable fixed points can be occasionally observed in random data, multiple approaches fitting these stringent criteria will not be seen.

In the implementation of these criteria, we excluded higher period behaviour (period 2, period 3, and so on), insisted that the geometry about the fixed point candidates be a flip saddle, and set criteria for the minimum acceptable linearity of the unstable manifold. We also set criteria for limits on the rates of approach and divergence of the trajectories. Because on these return plots it is easily shown that the eigenvalues (local rates of expansion and contraction along the respective manifolds) are simply the slopes of the respective manifolds, it is important to note that we found that the stable manifolds had negative slopes with magnitudes less than 1 and that the unstable manifolds had negative slopes with magnitudes greater than 1, further supporting the presence of chaos in these data (see Fig. 2).

Our chaos control technique begins with a learning phase consisting of the identification of unstable fixed points and the performance of local linear least-square fits to obtain the stable and unstable directions along with the rates of approach and divergence along them. The control phase consisted of waiting until the system executed a close approach to the unstable fixed point (within a small radius ε) along the stable direction, followed by an intervention that modified the timing of the predicted next interval in order to place it back onto the stable manifold. In this way we use the saddle structure inherent in the chaotic dynamics to bring the system back to the desired unstable fixed point with minimal intervention.

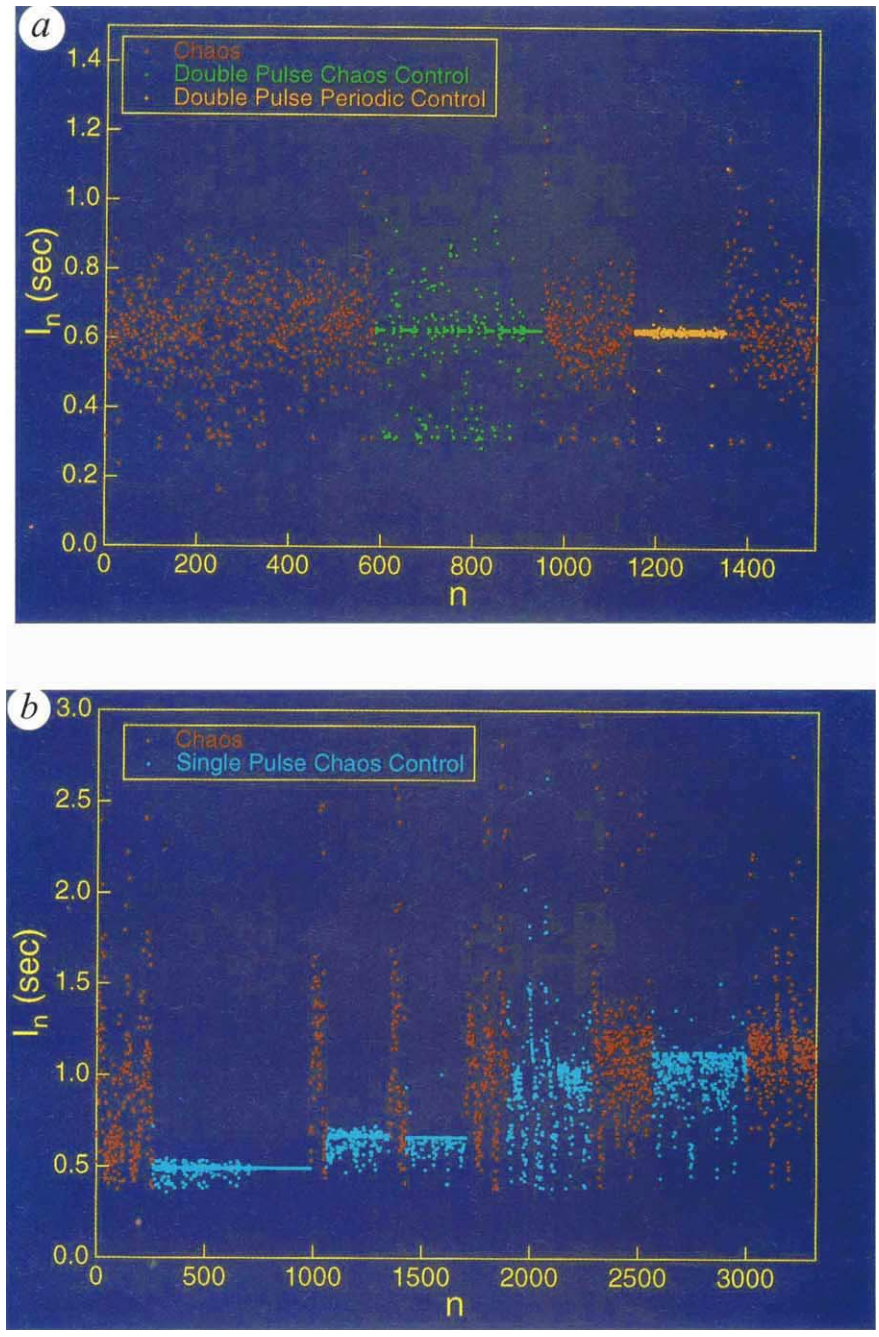

FIG. 5 Comparison of double-pulse chaos control (green) with double-pulse periodic pacing (orange) in an exceptional experiment where double-pulse chaos control was not very tight, and where double pulse periodic pacing was a better control method. Note the frequent escapes and recaptures of control with the chaos control method. This example helps illustrate how the chaos control method differed from overdrive periodic pacing. *b*, Experimental run where a wide range of control behaviours were observed. There are 5 sequential attempts to identify unstable fixed points and learn the manifold structure. Each control run is coded in blue. The first control run demonstrates what we classify as good control in Table 1. After relearning, the second attempt at control was also good, but at a higher fixed point (where the period of the underlying periodic orbit of the fixed point is larger). The third trial, despite learning nearly the identical fixed point as the previous trial, chose different manifolds and the control was not as good. We call such control runs, where intervals I_n larger than the fixed point are selectively eliminated partial control; note that this is a manifestation of the manifold selection and not just a function of the mean frequency of stimulation. This point is further clarified in the fourth and fifth control runs. The fourth control run selected a larger fixed point than the previous runs but control was a failure. The fifth and final control run of this sequence, despite selection of the highest fixed point of this series, achieved partial control with more adequate manifold and fixed-point selection.

In the following experiments, for periodic pacing, we used the same pulse interval as our calculated unstable fixed point. For anticontrol, we chose an interval that placed the next point on a line that was completely off the manifolds. We somewhat arbitrarily chose a direction that was the mirror image of the unstable manifold about the line of identity. This anticontrol technique proved effective in diverting the state of the system away from the stable direction and therefore from the unstable fixed point.

Experimental results

We did 91 experimental trials on 22 hippocampal slices from 9 rats. These trials consisted of combinations of chaos control, periodic pacing and anticontrol using both single and double stimulation pulses (Table 1). Double pulses were used at times to increase the effectiveness of stimulation.

Figure 1*b* shows an example of the synchronized burst discharges recorded extracellularly in CA3. The upper four traces show the burst discharges occurring at irregular intervals before control. On the fifth tracing chaos control pulses are delivered to the Schaffer collateral fibres, seen as large artefacts at the onset of a burst. Note that each control pulse can evoke a synchronized discharge in CA3, but control pulses are only given intermittently. As control becomes more stable, as seen most clearly on the bottom trace, the spontaneous bursts become increasingly periodic. We examined the relationship between burst intensity (duration, integrated amplitude and root mean

TABLE 1 Summary of experiments

	Chaos control		Periodic pacing		Anticontrol	
	Single	Double	Single	Double	Single	Double
Good	10	4	6	2	4	1
Partial	15	2	5	0	—	—
Bad	21	0	6	0	16	0
Total	46	6	17	2	20	1

square deviation) and interburst interval but found no correlations. The plot of the full series of these intervals before and during control is seen in the first half of the plot in Fig. 3.

Figure 1*c* shows 100 s of recording from the same experimental run before and after the initiation of periodic pacing. Note that now pulses immediately entrain the population bursts in the fifth tracing, but by the sixth tracing there is occasional escape behaviour evident when the population burst-fires just before the delivered pulses. The plot of the full series of these intervals before and during periodic pacing is seen in the second half of the plot in Fig. 3.

Figure 3 illustrates burst intervals before, during and after both single-pulse chaos control and single-pulse periodic pacing. Note that there is a qualitative difference in the control achieved with each method, as was seen from the traces of raw data shown in Fig. 1*b*, *c*.

Figure 4 compares the effects of anticontrol, double-pulse chaos control and single-pulse chaos control for another experiment. Here, the effect of anticontrol in reducing the periodicity of the preparation is clearly seen. We also demonstrated an increase in the effectiveness of double over single pulsing for this experiment.

Figure 5*a* illustrates an experiment where double-pulse chaos control and periodic pacing were compared, but the degree of control with chaos control was not as good as with periodic pacing. This experiment was exceptional, because most of the double-pulse experiments achieved very tight control (see Fig. 4, and summary in Table 1). Note that even with the increased stimulation of double pulsing, chaos control was not simply overdrive pacing, in that there were frequent escapes and recaptures of control consistent with the interactive control hypothesis.

Figure 5*b* illustrates the full gamut of results obtained with single-pulse chaos control. The first control trial demonstrated good control. Note that during this control sequence, the quality of the control improved. We then allowed the algorithm to relearn the fixed point and it chose one with a longer interval, again with good control. Whether this is a manifestation of the non-stationary nature of the system, or truly reflects the presence of multiple unstable period 1 fixed points is unclear. Relearning a third time, the algorithm selected different manifolds without substantially changing the value of the fixed point, but the control is not as good. This third control run exhibited what we call partial control in the results shown in Table 1; in partial control, manifold selection was not optimal, and time intervals longer than those of the chosen fixed-point interval appear eliminated. Relearning a fourth time, a fixed point is chosen at a longer interval than the previous three attempts. This was a control failure. Nevertheless, relearning a fifth time with an even longer fixed-point interval gave partial control. This sequence demonstrates that the quality of control is not simply a function of the frequency chosen, the control is critically dependent on the quality of the fixed points and manifolds selected.

Discussion

This is the second attempt at achieving control of a chaotic biological system[8] with a derivative method of Ott, Grebogi and Yorke[1]. The observation of small-scale structure and the identification of stable and unstable manifolds near unstable fixed points for many of these burst-firing slices demonstrated the presence of deterministic chaos in this simple neuronal system. For this preparation, complicated control theory is not required just to achieve relatively fast periodic behaviour. Above certain frequencies, periodic pacing was effective in entraining the spontaneous burst discharges in CA3. However, the quality of control with periodic pacing was not equivalent with the chaos control method; furthermore, the chaos control method has the advantage over overdrive periodic pacing in terms of its ability to identify and track fixed points over time. In addition, the control of chaos strategy offers the ability to break up fixed-point behaviour with anticontrol. The anticontrol method used here uses a minimal number of stimuli needed to prevent periodic behaviour.

Although it was easy to observe the unstable manifolds from this preparation, it was difficult to place accurately the stable manifold. This is because the system has many degrees of freedom (that is, is high dimensional), and the expectation of fully disentangling its dynamics with a two-dimensional embedding is simplistic. In addition, increasing amounts of noise in a system will increase the frequency of escapes from control and eventually render control impossible[1]. Despite these difficulties, good or partial control could frequently be achieved with our implementation of chaos control. The application of new theoretical techniques recently developed for the control of high dimensional systems[23] could improve the reliability of control for such neuronal preparations.

We experimented with several variants of stimulation delivery. In addition to single pulses, double pulses were used and were often more effective in achieving higher quality control. We also explored limiting the delivery of control pulses by prohibiting consecutive control pulses without an intervening spontaneous burst. This latter method was less effective than permitting consecutive pulsing.

Because this neuronal preparation shares similar characteristics with epileptic interictal spike foci, we believe these methods may be applied to such foci. Although it is impossible to predict what effect increasing the periodicity of epileptic foci will have, the opposite effect of breaking up fixed-point periodic behaviour with anticontrol could be a more useful intervention. □

Received 11 May; accepted 5 July 1994.

1. Ott, E., Grebogi, C. & Yorke, J. A. *Phys. Rev. Lett.* **64,** 1196–1199 (1990).
2. Shinbrot, T., Grebogi, C., Ott, E. & Yorke, J. A. *Nature* **363,** 411–417 (1993).
3. Ditto, W. L., Rauseo, S. N. & Spano, M. L. *Phys. Rev. Lett.* **65,** 3211–3214 (1990).
4. Hunt, E. R. *Phys. Rev. Lett.* **67,** 1953–1955 (1991).
5. Roy, R., Murphy, T. W., Maier, T. D. & Gills, Z. *Phys. Rev. Lett.* **68,** 1259–1262 (1992).
6. Petrov, V., Gaspar, V., Masere, J. & Showalter, K. *Nature* **361,** 240–243 (1993).
7. Rollins, R. W., Parmananda, P. & Sherard, P. *Phys. Rev.* E**47,** R780 (1993).
8. Garfinkel, A., Spano, M., Ditto, W. L. & Weiss, J. *Science* **257,** 1230–1235 (1992).
9. Gotman, J. *Can. J. neurol. Sci.* **18,** 573–576 (1991).
10. Katz, A., Marks, D. A., McCarthy, G. & Spencer, S. S. *Electroenceph. clin. Neurophysiol.* **79,** 153–156 (1991).
11. Pedley, T. A. & Traub, R. D. in *Current Practice of Clinical Electroencephalography* 2nd edn (eds Daly, D. D. & Pedley, T. A.) 107–137 (Raven, New York, 1990).
12. Rutecki, P. A., Lebeda, F. J. & Johnston, D. *J. Neurophysiol.* **54,** 1363–1374 (1985).
13. Korn, S. J., Giacchino, J. L., Chamberlin, N. L. & Dingledine, R. *J. Neurophysiol.* **57,** 325–341 (1987).
14. Traynelis, S. F. & Dingledine, R. *J. Neurophysiol.* **59,** 259–276 (1988).
15. Traub, R. D. & Dingledine, R. *J. Neurophysiol.* **64,** 1009–1018 (1990).
16. Traub, R. D. & Miles, R. *Neuronal Networks of the Hippocampus* (Cambridge Univ. Press, Cambridge, 1991).
17. Chang, T., Schiff, S. J., Sauer, T., Gossard, J.-P. & Burke, R. E. *Biophys. J.* **67,** 671–683 (1994).
18. Schiff, S. J., Jerger, K., Chang, T., Sauer, T. & Aitken, P. G. *Biophys. J.* **67,** 684–691 (1994).
19. Jefferys, J. G. R. *J. Physiol.* **319,** 143–152 (1981).
20. Durand, D. *Brain Res.* **382,** 139–144 (1986).
21. Kayyali, H. & Durand, D. *Expl Neurol.* **113,** 249–254 (1991).
22. Ott, E. *Chaos in Dynamical Systems* (Cambridge Univ. Press, Cambridge, 1993).
23. Auerbach, D., Grebogi, C., Ott, E. & Yorke, J. A. *Phys. Rev. Lett.* **69,** 3479–3482 (1992).

ACKNOWLEDGEMENTS. We thank P. G. Aitken for his invaluable teaching and advice and S. Mahan for research assistance. We gratefully acknowledge support from an NIMH grant (S.J.S.), the Children's Research Institute (S.J.S. and T.C.), an Office of Naval Research Young Investigator Award (W.L.D.), the Naval Surface Warfare Center's Independent Research Program (M.L.S.) and the Physics Division of the Office of Naval Research (M.L.S. and W.L.D.) The contribution of software from Manugistics Inc. is greatly appreciated.